Document embedding centroids: new and versatile semantic descriptors for compounds

John P. Santa Maria Jr, Scott Gleim, Eugen Lounkine, & Jeremy Jenkins

Abstract

Language embedding models facilitate learning on unstructured text by encoding entities of interest in a vector space. Here we demonstrate how document embedding models applied to Pubmed abstracts can be used to generate descriptors for compounds. These descriptors facilitate tasks such as nearest neighbor retrieval. We demonstrate that semantic embeddings encode orthogonal information when compared to traditional chemical topological and biological descriptors and posit that the integration of semantic embeddings into ligand-based virtual screening pipelines will enable future lead identification in early drug discovery.

Introduction

Biomedical data is being generated at unprecedented scale. This poses a challenge for the evidence-based prioritization of therapeutic, disease, and/or target relationships in early drug discovery. Though pharmacogenomic databases facilitate the cataloguing of scientists' accumulated knowledge, their utility and accuracy are limited by several factors. First, all databases rely on ontologies, which do not always capture relevant entities/relationships and may not translate across applications. Furthermore, some databases rely on manual curation, which can be expensive, time-intensive, and subject to human interpretations and errors. Finally, gaps in data incorporation may lead to missing or incorrect information. One way to address these limitations and improve evidence integration is to learn entity associations directly from the unstructured text of primary research articles and experimental records.

The development of word and document embedding models has facilitated rapid, automated knowledge extraction and downstream learning from unstructured text [1,2]. These techniques work by encoding texts as numeric vectors based on semantic content and/or contexts. Subsequent similarity and analogy relationships between text entities can then be gleaned using simple algebraic and arithmetic operations, while classification learning can be facilitated using the reduced dimensionality of vector representations. Semantic embeddings have been applied to answer diverse biomedical research questions, such as learning disease-drug and disease-disease relationships from research articles and clinical notes [3, 4], predicting compound-protein, protein-protein, and gene-disease interactions [5, 6], and predicting material functional properties [7].

The automated generation and comparison of descriptive fingerprints for compounds can facilitate diverse classification tasks for drug discovery. For example, calculated similarity in chemical feature space can help identify new target modulators in quantitative structure activity relationship (QSAR) modeling [8], and similarity between assay performance profiles can facilitate mechanism-of-action deconvolution [9]. Previous work has demonstrated that augmenting traditional chemical structural fingerprints with semantic occurrence information can benefit classification performance [10]. We expand upon this idea, creating and comparing several different methods for generating semantic descriptors of compounds. We demonstrate that chemical semantic fingerprints can be generated rapidly from public biomedical literature and have utility for compound nearest neighbor retrieval. We also show that the document centroid method captures partially orthogonal information in comparison to existing biological and chemical fingerprints.

Methods

Semantic modeling

Abstracts from NCBI/Pubmed through March 2020 were assembled into a joint corpus for semantic modeling. Document embeddings were also generated using the Universal Sentence Encoder Multilingual Model [11]. In order to assess model quality, we developed an information retrieval task similar to that of Le & Mikolov [2]. We assembled query sets of the top 10 NCBI Pubmed search results for random Medical Subject Heading (MESH) terms. For each query a triplet was assembled containing two abstracts from the query and a random third abstract. Pairwise relatedness was then calculated within triplets.

Fingerprint generation, similarity calculation, and clustering

Compound semantic fingerprints generated using the document embedding centroid method were calculated by summing the vectors of documents in which the compounds occur, followed by L2-normalization. Semantic fingerprints using the TFIDF method were calculated as reduced 300-dimensional vectors by principal component analysis of the TFIDF matrix, performed using the python package delayedsparse [12]. Similarity for each method was calculated using the cosine metric. Normalized pointwise information (nPMI) between two compounds, *A* and *B* was calculated using the following formula:

$$nPMI = \frac{\ln(cooccur(A,B) * N / (occur(A) * occur(B)))}{-\ln(cooccur(A,B)/N)} \quad [13]$$

Compound occurrences in Pubmed articles were obtained using a combination of public and private curation tools, including Pubtator and Leadmine (https://www.nextmovesoftware.com/leadmine.html) [14]. Chemical similarity was calculated using the tanimoto metric from Morgan fingerprints of radius 2 generated using RDKit (fpsize=2048 bits). Biological similarity was calculated using pearson correlations of 722-dimensional compound vectors comprising normalized z-scores of activities in Novartis high-throughput assays, as previously described [9].

DrugBank categories and drug-target association modeling

Category labels for drugs (such as antibiotics or antineoplastics) were retrieved from DrugBank [15]. Human protein associations were obtained from a combination of Chembl, Reaxys, GVK, and Clarivate Integrity databases for 100 random proteins possessing at least 10 unique compounds with association strength >= 3 as defined in [16]. Each fingerprint type was assessed for nearest neighbor retrieval by calculating a leave-one-out, cross-validated ROC AUC metric: 100 ranked nearest neighbors were retrieved for each member of the drug category or target; area under the curve (AUC) was calculated for the sensitivity/specificity curve of retrieval of the remaining category members at each rank threshold; the resulting AUCs were then averaged for each category/target. Nearest neighbors retrieved using the co-occurrence scoring method were ranked using scaled mutual information.

Results

Document embedding models can capture latent semantic content for input corpora. We hypothesized that part of this encoded meaning includes information about compounds mentioned within text, and that we could map a compound into semantic space by calculating the centroid of the document vectors in which it occurs (**Figure 1A**). To first assemble document embeddings, we employed the pre-trained Universal Sentence Encoder multilingual model on ~14.6M Pubmed abstracts [11]. We assessed the quality of the document embeddings using a derived Information Retrieval task, and obtained an accuracy of 90.5%, a 26.4% improvement over a bag-of-words approach (**Supplementary Table 1**). Visual inspection of top document-document cosine scores also revealed highly similar texts (**Supplementary Table 2**). These data gave us confidence in the quality and utility of document embeddings generated for a corpus of Pubmed abstracts, and supported the applicability of the universal sentence encoder algorithm within the technical domain of biomedical literature.

In order to assemble semantic representations of molecules, we next obtained the occurrences of 1.35M compounds within 8.9M Pubmed articles. Compound embeddings were then generated as the unweighted average of the document vectors in which they occurred, resulting in a 512-dimensional representation within the span of the document space. Semantic relatedness between compounds was calculated as a cosine score between their vectors, with a maximum value of 1 representing a compound's similarity with itself. As an example, we applied our document centroid (DC) method for 3 common drugs (**Table 1**). For comparison, we generated results using two alternative measures of compound-compound semantic relatedness: normalized pointwise mutual information (nPMI), and a vector representation of equivalent dimensionality derived from the compound-document TF-IDF matrix (see Methods). We observed overlaps in the nearest neighbors retrieved using each method, supporting the ability of our approach to quantify and rank semantic similarity. We noted for each query that the top neighbors produced using the document centroid method were of related drug class and were among the most co-occurring compounds. In contrast, we noted that the order of retrieval, magnitude of calculated similarity metrics, and number of cooccurrences diverged among the three methods. To quantify this more directly, we considered the distributions of similarity scores (Fig 1B). The cosine similarity metric for document centroids followed a normal distribution centered approximately at 0 with a long right tail, while TFIDF similarity is negatively-skewed with a sharp peak near 1 and nPMI has a sparse distribution with a sharp peak at -1. A nPMI score of -1 is realized when two compounds do not co-occur, and the sharp peak in this score distribution reflects the rarity of co-occurrence between random pairs of compounds in our dataset. In contrast, both TFIDF and DC methods generate similarity measures for compound pairs using the likeness of their textual contexts even if the pair has not explicitly co-occurred in documents. This feature further supports the utility of these methods for discovery hypothesis generation. Finally, in examining the relationship between similarity metrics and compound co-occurrence, we observed a modest correlation (Pearson: DC=0.29 p~0, TF-IDF=0.15 p~0), supporting that compounds with a high similarity metric share significant semantic relationships.

Table 1: Top 5 nearest neighbors retrieved using each method of semantic similarity for 3 example drug queries

	DC				TFIDF				nPMI			
Query	Neighbor	Sim	Rank	Cooccur.	Neighbor	Sim	Rank	Cooccur.	Neighbor	Sim	Rank	Cooccur.
Imatinib	imatinib	1	1	-	imatinib	1	1	-	imatinib	1	1	-
	nilotinib	0.809	2	1725	nilotinib	0.995	2	1725	nilotinib	0.721	2	1725
	dasatinib	0.763	3	2013	n-desmethyl imatinib	0.994	3	54	dasatnib	0.697	3	2013
	ponatinib	0.656	4	271	dasatinib	0.990	4	2013	bosutinib	0.573	4	330
	bosutinib	0.647	5	330	(E)-2-(2-Methoxy-5-((2,4,6-trimethoxystyrylsulfonyl)methyl)phenyl amino)propanoic acid	0.990	5	11	sunitinib	0.561	5	1519
Lenalidomide	lenalidomide	1	1	-	lenalidomide	1	1	-	lenalidomide	1	1	-
	pomalidomide	0.844	2	421	medphalan	0.695	2	443	thalidomide	0.785	2	2853
	thalidomide	0.830	3	2853	vadimezan	0.370	3	4	pomalidomide	0.745	3	421
	bortezomib	0.821	4	1664	carmustine	0.243	4	72	bortezomib	0.713	4	1664
	carfilzomib	0.735	5	251	melphalan	0.224	5	345	carfilzomib	0.648	5	251
Penicillin V	penicillin V	1	1	-	penicillin V	1	1	-	pencillin V	1	1	-
	penicillin G	0.770	2	812	cilligen	0.897	2	2	2-nitro-5-[(phenoxyacetyl)amino] benzoic acid	0.597	2	31
	amoxicillin	0.715	3	425	6-aminopenicillanic acid	0.885	3	43	4-hydroxypencillin V	0.565	3	3
	cefalexin	0.687	4	96	benzylpenicilloyl polylysine	0.873	4	2	(6R,7R)-3-Chloro-7-[[2-(5-chloro-1-benzothiophen-3-yl)acetyl]amino]-8-oxo-5-thia-1-azabicyclo[4.2.0]oct-2-ene-2-carboxylic acid	0.565	3	3
	cloxacillin	0.670	5	104	penilloic acid	0.860	5	1	phenoxyacetic acid	0.550	5	2

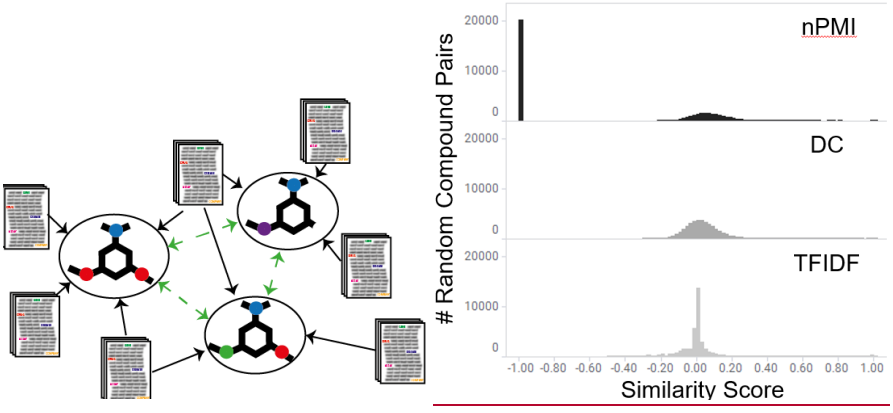

Figure 1: A) Overview of DC method. A compound is represented as the centroid of all document vectors representing its literature occurrences. B) Similarity score distributions for 120K random compound pairs using three different methods of semantic relatedness.

Nearest neighbor retrieval performance of document centroids for targets and compound classes

Compound descriptors often have utility in predicting biological activities for compounds. We wondered how the retrieval and classification power of descriptors generated using DC compared to more traditional chemical and biological assay-based descriptors. To investigate this, we devised two common tasks, drug mechanism-of-action and target association categorization, and evaluated the performance of each descriptor by determining how many of the retrieved nearest neighbors of category members reside within the category. We obtained ~140 categorizations of drugs from the Drugbank database and assessed the performance of each descriptor type in random forest modeling (see Methods). We observed that DC descriptors exhibited an average ROC AUC across drug categories of 0.661, far outperforming simple co-occurrence ranking, biological descriptors, and random (ROC AUC=0.5), and performing similar to the chemical descriptor (**Figure 2A**). In investigating individual categories, we observed differing best performing descriptors for each category, and that several classes were best predicted using DC (**Figure 2B**, Supplemental Dataset 1). We next compared descriptor performance in predicting compound-target associations using data for 100 human target proteins obtained from Chembl and other public pharmacogenomic databases (see Methods). DC descriptors achieved a ROC AUC score of 0.695 across all targets, outperforming co-occurrence ranking, chemical and biological descriptors, and random (**Figure 2C**). In investigating individual targets, we again observed that while no individual descriptor was universally optimal, DC performed best for several targets (**Figure 2D**). Though we observed no correlation between ROC AUC metrics and compound occurrence frequency in literature for Drugbank categorizations, we did observe a modest negative correlation (-0.23, p=$1e^{-307}$) between target ROC AUC scores and the logarithm of occurrence for target associations (**Supplemental Figure 2**). These data support the ability of semantic descriptors, generated using document embedding centroids, to facilitate compound nearest neighbor retrieval tasks.

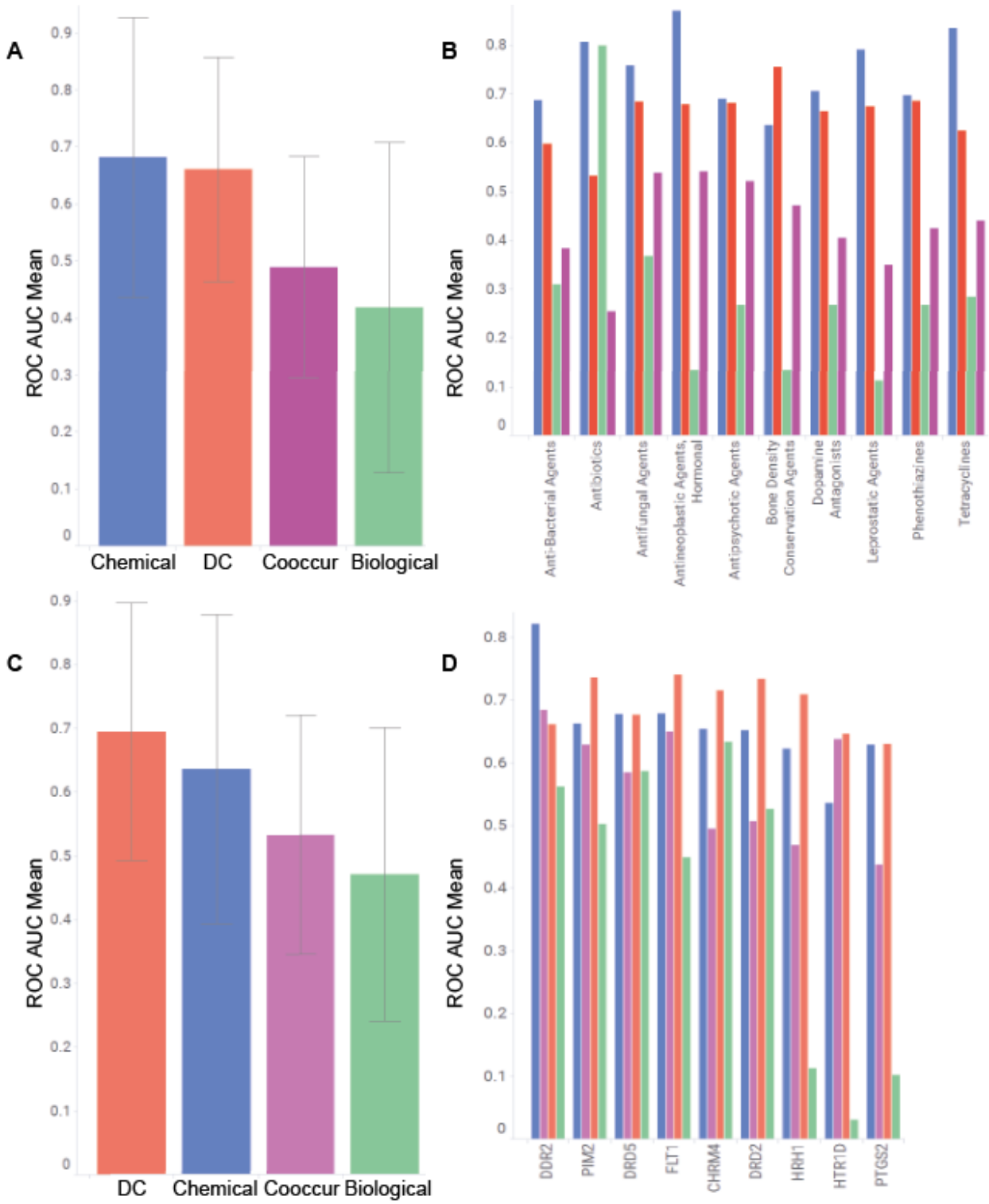

Figure 2: Classification performance of DC for drug mechanism-of-action and drug target tasks. A) Average ROC AUC of each descriptor method across 100+ Drugbank categories B) Example ROC AUC scores averaged across category members for each descriptor method. C) Average ROC AUC of each descriptor method across 100 random human target proteins D) Example ROC AUC scores averaged across compounds associated with a given target for each descriptor method. Note that illustrated

examples only display the categories that possess compounds with descriptors for all methods. Error bars represent +/-1 standard deviation.

The difference in performance between semantic, biological, and chemical descriptors during the classification tasks is a direct result of differences in calculated similarity between compound class members. To investigate this in more detail, we looked at the correlation between calculated similarity measures among random pairs of compounds (**Figure 3**). We observed no significant correlation between each similarity measure, supporting the orthogonality of these three descriptor types for compounds. We observed distribution outliers and examined several of these compound pairs in further detail (**Table 2**). For example, compounds 1 and 2 have conserved molecular features contributing to their high chemical similarity score, but occur in distinct semantic contexts (the former reported as an anti-allergic [17] and the latter as a component of metallocycles [18]). In contrasts, compounds 3 (Grassofermata) and 4 (Lipofermata) co-occur as identified inhibitors of a fatty acid transporter [19], but have distinct chemical structures and poorly correlated performance in internal Novartis biological assays. Together, our observations on DC nearest neighbor retrieval and orthogonality to other compound similarity metrics suggest that semantic similarity may have utility in scaffold hopping.

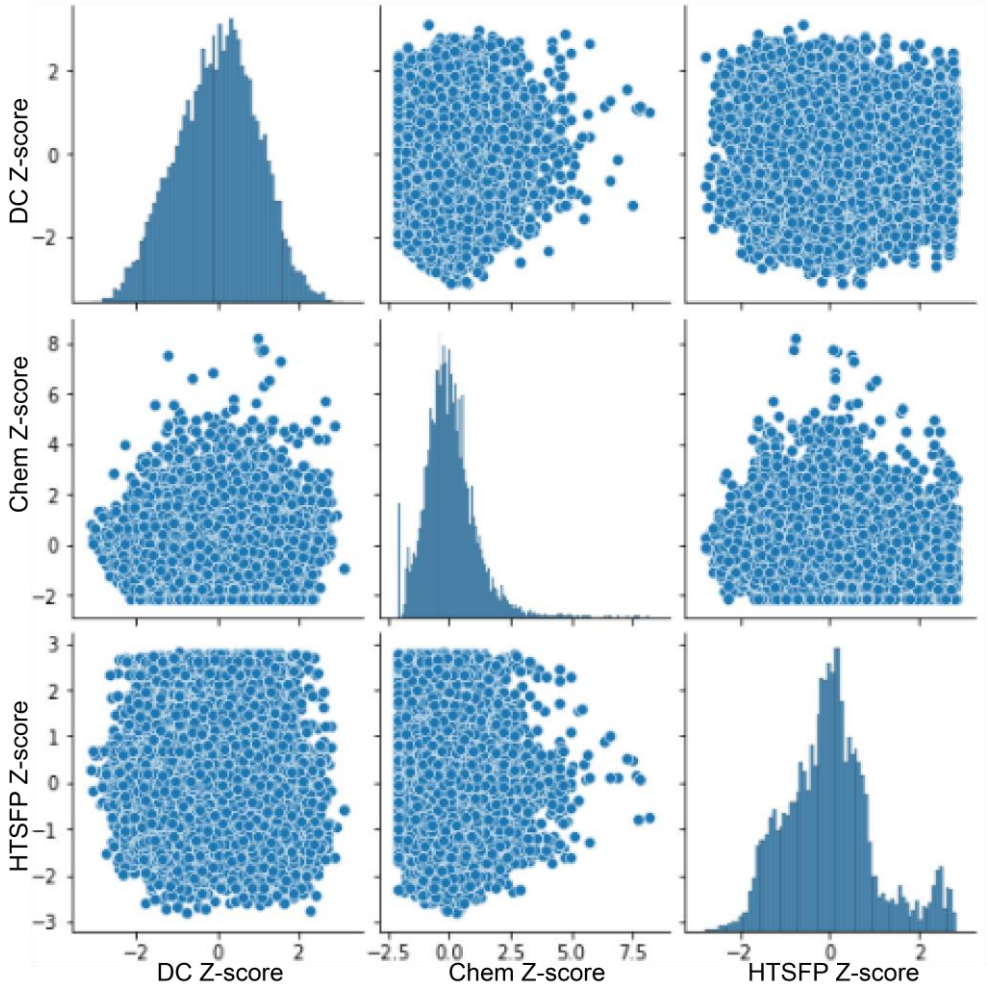

Figure 3: Correlogram illustrating the relationships between semantic, chemical, and biological similarity metrics for random compound pairs. Example pairs are described in further detail in **Table 2**.

Conclusions

Numerous fingerprinting methods have been developed to describe compounds and their characteristics. These methods aim to make compound characteristics computable and predictable, in order to facilitate drug discovery, but they often possess orthogonal information in comparison to one another [20]. We propose document centroids as a novel method to generate descriptors for compounds by capturing their semantic contexts. We demonstrated that DC outperforms simple co-occurrence and mutual information standards for semantic relatedness. We also showed that these descriptors facilitate the comparison of compounds to one another. As other entity types can also be extracted automatically from scientific literature, our method may serve as a general framework to embed entities within a common semantic space for cross-domain comparisons.

The construction of semantic descriptors for compounds is inherently dependent on their occurrence in literature. This serves as both a strength and a weakness – as the scientific literature grows, semantic representation of compounds becomes better informed, but literature biases and inaccuracies as well as the ability of automated entity recognition methods to correctly identify occurrences, may limit accuracy. Nevertheless, our methods are widely implementable using current public data and can rapidly integrate newly published articles and compounds in either public or proprietary domains. Alternative literature sources (such as patents or popular chemistry blogs) may also serve to improve the quality and breadth of our semantic space.

Table 2: Example Similarity Scores (Z-scores) for Compound Pair Distribution Outliers

Molecule1	Molecule2	ChemSim	HTSFPSim	DCSim
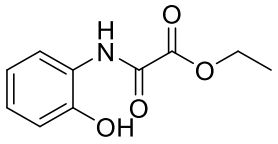 (1)	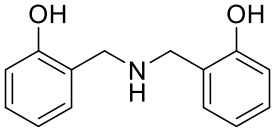 (2)	0.289 (4.00)	0.592 (-0.16)	0.063 (-2.31)
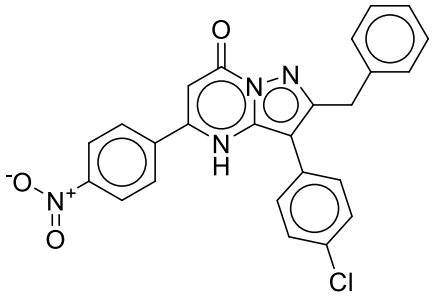 (3)	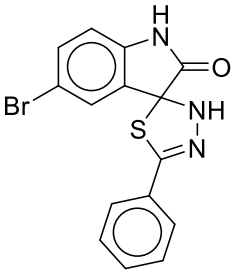 (4)	0.106 (0.126)	0.285 (-2.417)	0.557 (0.550)

References

1. Mikolov, T., Sutskever, I., Chen, K., Corrado, G., & Dean, J. “Distributed Representations of Words and Phrases and their Compositionality”. *ArXiv* (2013) arXiv:1310.4546 [cs.CL].
2. Le, Q., Mikolv, T. “Distributed Representation of Sentences and Documents”. *ArXiv* (2014) arXiv:1405.4053 [cs.CL].
3. Muneeb, T.H., Sahu, S.K., & Anand A. “Evaluating distributed word representations for capturing semantics of biomedical concepts”. *Proc ACL-IJCNLP* (2015). pp. 158-163.
4. Beam, A.L., *et al.* “Clinical concept embeddings learned from massive sources of multimodal medical data”. *ArXiv* (2019) arXiv:1804.01486 [cs.CL].
5. Wan, F. & Zeng, J. “Deep learning with feature embedding for compound-protein interaction prediction”. *bioRxiv* (2016)
6. Smaili, F.Z., Gao, X., & Hoehndorf, R. “OPA2Vec: combining formal and informal content of biomedical ontologies to improve similarity-based prediction” *Bioinformatics* (2018) 34(13):i52-i60.

7. Tshitoyan, V., *et al.* "Unsupervised word embeddings capture latent knowledge from materials science literature". *Nature* (2019) 571: 95-98.
8. Wilkins, C.L. & Randić M. "A graph theoretical approach to structure-property and structure-activity correlations". *Theoret Chim Acta* 1:45-68.
9. Wasserman, A.M., *et al.* "A screening pattern recognition method finds new and divergent targets for drugs and natural products". *ACS Chem Biol* (2014). 9: 1622-1631.
10. Wan, F. & Zeng, J.M. "Deep learning with feature embedding for compound-protein interaction prediction". *bioRxiv* (2016). bioRxiv 086033; doi:10.1101/086033.
11. Yang, Y., *et al.* "Multilingual Universal Sentence Encoder for Semantic Retrieval". *arXiv* (2019). arXiv:1907.04307 [cs.CL].
12. Niitsuma, H. & Lee, M. "Word2Vec is a special case of Kernel Correspondence Analysis and Kernels for Natural Language Processing". *arXiv* (2018). arXiv:1605.05087[cs.LG].
13. Role, F. & Nadif, M. "Handling the impact of low frequency events on co-occurrence based measured of word similarity – a case study of pointwise mutual information". (2011) In Proceedings of the International Conference on Knowledge Discovery and Information Retrieval - Volume 1: KDIR, (IC3K 2011) ISBN 978-989-8425-79-9, pp 218-222.
14. Wei, C-H., Allot, A., Leaman, R., & Lu, Z. "PubTator central: automated concept annotation for biomedical full text articles". *Nucl Acid Res* (2019). 47(W1):W587-W593.
15. Wishart DS, Feunang YD, Guo AC, Lo EJ, Marcu A, Grant JR, Sajed T, Johnson D, Li C, Sayeeda Z, Assempour N, *et al*. "DrugBank 5.0: a major update to the DrugBank database for 2018". *Nucleic Acids Res.* (2018). 46(D1):D1074-D1082
16. Wang, Y., *et al*. "Evidence-Based and Quantitative Prioritization of Tool Compounds in Phenotypic Drug Discovery". *Cell Chem Biol* (2016). 23(7):862-874.
17. Sellstedt, JH, *et al*. "Oxanilic acids, a new series of orally active antiallergic agents". *J Med Chem* (1975). 18(9):926-933.
18. Xu, M-Y., *et al.* "Aggregation of the metallocycles $\{Cu_8\}$ and $\{Cu_{20}\}$ using [Cu(bp)] units (H_2bp =bis(2-hydroxybenzyl)amine): structures and magnetic properties". *Dalton Trans*. (2016). 45(12):4993-4997.
19. Black, P.N., *et al.* "Fatty acid transport proteins: targeting FATP2 as a gatekeeper involved in the transport of exogenous fatty acids". *MedChemComm.* (2016). 7:612-622.
20. Bender, A., *et al.* "How similar are similarity searching methods? A principal component analysis of molecular descriptor space". (2009). *J Chem Inf Model* 49:108-119.

Supplementary Table 1. **Accuracy in a Pubmed search information retrieval task**

Model	**Accuracy**
Bag of Words	64.1
USE-ML	**90.5**
USE_large	85.4

Supplementary Table 2. **Example high similarity abstracts from our Pubmed Doc2Vec Model**

PMID1	PMID2	Sim	Abstract 1	Abstract 2
3492961	3568594	0.860	Susceptibility testing of 7,775 recent clinical isolates from four medical centers showed Ro 15-8074 to be 2- to greater than 8-fold more active than either cefaclor or cefuroxime against the Enterobacteriaceae. Ro 15-8074 MICs for 50% of the strains tested were greater than or equal to 32 micrograms/ml for Staphylococcus spp., enterococci,	The susceptibility testing of 7,745 recent clinical isolates from four medical centers showed Ro 19-5247 to be eight- to greater than 64-fold more active than cephalexin against the Enterobacteriaceae. Ro 19-5247 was comparable with cephalexin in anti-staphylococcal activity (MIC50, 4.0 micrograms/ml) and fourfold more active than cefixime. None of the oral cephalosporins were effective (MIC50,

			Pseudomonas aeruginosa, and Pseudomonas maltophilia. beta-Lactamase hydrolysis experiments failed to demonstrate significant Ro 15-8074 inactivation by commonly encountered chromosomal or plasmid-mediated enzymes (P99, K1, K14, TEM, and CARB).	greater than 32 micrograms/ml) against enterococci, Pseudomonas aeruginosa and P. maltophilia. beta-lactamase hydrolysis experiments failed to demonstrate significant Ro 19-5247 inactivation by ten commonly encountered chromosomal- or plasmid-mediated enzymes (P99, K1, K14, TEM, CARB, OXA).
8022066	8283890	0.850	In this study, we evaluated cardiac myocyte viability and function under hypothermic conditions using three types of storage solutions; saline solution (SS), Euro-Collins solution (ECS) and MCDB 107 medium (MM). Cardiac myocytes were isolated from neonatal rat ventricles by collagenase dispersion and cultured for 4 days with MCDB 107 medium. A total of 12.5 x 10(5) myocytes/culture dish were used and the myocytes were incubated at 4 degrees C for 6, 12, 18 and 24 hrs in the various storage solutions. After each incubation time, CPK and LDH were measured in the storage solutions. The myocytes were then cultured in MCDB 107 medium and incubated for 24 hrs at 37 degrees C to evaluate the recovery of the myocyte beating rate. In group MM (n = 7), the recovery ratio of the myocyte beating rate was 99.2 percent of control (beating rate prior to hypothermic incubation) at 6 hours, 104.6% at 12 hrs and 44.8% at 24 hrs. Groups SS and ECS (n = 7 each) had significantly lower recovery ratios than the MM group (at 6 hrs: 74.3, 34.0; at 12 hrs: 61.0, 32.2; at 24 hrs: 0.0, 0.0 percent of control, respectively). Release of CPK and LDH in the MM group gradually increased and at 24 hrs was 28.6 IU/l and 93.6 IU/l, respectively. However, the SS group had significantly increased CPK and LDH values at 24 hrs (CPK: 66.9, LDH: 164.2). The ECS group showed the greatest increase in both markers (CPK: 317.5, LDH: 421.2). In summary, saline solution showed a beneficial effect on recovery of myocyte viability at 12 hours compared to Euro-Collins solution, however, MCDB 107 medium had the best overall protective effect on cultured myocytes. Accordingly, alternate hypothermic storage solutions, such as cell-culture medium, may have protective characteristics that are suitable for cardiac preservation.	In this study, we evaluated cardiac myocyte viability and function under hypothermic conditions with four types of storage solutions, saline solution, Euro-Collins solution, University of Wisconsin solution, and MCDB 107 medium. Cardiac myocytes were isolated from neonatal rat ventricles by collagenase dispersion and cultured for 4 days with MCDB 107 medium. A total of 12.5 x 10(5) myocytes per culture dish was used and the myocytes were incubated at 4 degrees C for 6, 12, 18, and 24 hours in the various storage solutions. After each incubation time, creatine kinase and lactate dehydrogenase were measured in the storage solutions. The myocytes were then incubated for 24 hours at 37 degrees C to evaluate the recovery of the myocyte beating rate. In the MCDB 107 group (n = 7), the recovery ratio of myocyte beating rate was complete by 12 hours, then decreased to 44.8% of control (beating rate before hypothermic incubation) at 24 hours. The saline, Euro-Collins, and University of Wisconsin groups (n = 7 each) had significantly lower recovery ratios than the MCDB 107 group (at 12 hours: 61.0%, 32.2%, and 48.9%; at 18 hours: 0.0%, 5.5%, and 15.1% of control, respectively). Release of creatine kinase and lactate dehydrogenase in the MCDB 107 group gradually increased and at 24 hours was 143.2 mIU/flask and 486.2 mIU/flask, respectively. However, the saline and University of Wisconsin groups had significantly increased creatine kinase and lactate dehydrogenase values at 24 hours (creatine kinase: 334.6 and 319.6 mIU/flask; lactate dehydrogenase: 821.6 and 654.4 mIU/flask, respectively). The Euro-Collins group showed the greatest increase in both markers (creatine kinase: 1587.5, lactate dehydrogenase: 2106.9 mIU/flask). In summary, saline and University of Wisconsin solutions showed a beneficial effect on recovery of myocyte viability at 12 hours compared with Euro-Collins solution, however MCDB 107 medium had the best overall protective effect on cultured myocytes. Accordingly, alternate hypothermic storage solutions, such as cell-culture medium, may have protective characteristics that are suitable for cardiac preservation.
23217281	23053265	0.732	*BACKGROUND:* To evaluate the efficacy and tolerability of capecitabine combined	*PURPOSE:* The aim of this study was to evaluate the efficacy and safety of irinotecan

			with thalidomide in patients with advanced pancreatic cancer (APC) who have previously received gemcitabine-based therapy. *METHODS:* A total of 31 patients were recruited prospectively in Shandong Tumor Hospital from May 2007 to April 2009. Capecitabine was offered to patients twice a day at a dose of 1250 mg/m(2) for 14-day then followed by 7-day rest. Thalidomide was administered 100 mg/day without interruption until disease progression or occurrence of unacceptable toxicity. *RESULTS:* Two patients presented partial response (PR), 11 patients showed stable disease (SD) and eighteen patients presented progressive disease (PD). The median progression-free survival (PFS) was 2.7 months (95% confidence interval (CI), 2.4-3.3) and the median overall survival (OS) was 6.1 months (95% CI, 5.3-6.9). In the subgroup analysis, PFS had a significant difference between the serum CA19-9 level decreasing >25% and decreasing <25%, with 3.0 months (95% CI, 2.5-3.6) and 2.5 months (95% CI, 1.8-3.2), (Log Rank = 0.02), respectively. Hematological toxicity included leukocytopenia, anemia and neutropenia. Non-hematological toxicities included diarrhea, skin rash, nausea/vomiting, hand-foot syndrome, fatigue, dizziness, drowsiness and constipation. *CONCLUSION:* Capecitabine combined with thalidomide is a well-tolerated second-line regimen, in patients with APC refractory to gemcitabine.	monotherapy in patients with advanced pancreatic cancer (APC). *METHODS:* Patients with APC refractory to gemcitabine and S-1 were included. Irinotecan (100 mg/m(2)) was administered on days 1, 8, and 15 every 4 weeks until disease progression or unacceptable toxicity was observed. The relationship between uridine diphosphate glucuronosyl transferase 1 family polypeptide A1 gene (UGT1A1) polymorphisms and clinical outcomes was evaluated. *RESULTS:* Between January 2007 and December 2011, 231 cycles were delivered in 56 patients. Irinotecan was administered as second-line chemotherapy in 35.7% of patients and as third-line chemotherapy or later in 64.3%. A partial response was achieved in two (3.6%) and stable disease in 23 patients (41.0%), giving a disease control rate of 44.6%. The median time to progression (TTP) and overall survival (OS) were 2.9 (95% confidence interval [CI] 1.8-3.5) months and 5.3 (95% CI 4.5-6.8) months, respectively. Median survival from the first-line chemotherapy was 19.5 (95% CI 15.3-23.8) months. Major grade 3/4 adverse events included neutropenia (28.6%), anemia (12.5%), and anorexia (10.7%). Patients with *6 and/or *28 allele(s) (n = 15) were associated with grade 3/4 neutropenia and anorexia but showed longer TTP (5.3 vs. 1.8 months; p = 0.05), and OS (8.0 vs. 4.8 months; p = 0.09) than those without *6 and/or *28 (n = 29). *CONCLUSIONS:* Salvage chemotherapy with irinotecan was moderately effective and well-tolerated in patients with APC refractory to gemcitabine and S-1. UGT1A1 polymorphisms were associated with toxicity and efficacy.
10527334	23724179	0.679	*BACKGROUND AND OBJECTIVES:* The purpose of the present study was to evaluate the results of diagnostic laparoscopy in children with chronic recurrent abdominal pain. *PATIENTS AND METHODS:* Thirteen children with chronic recurrent abdominal pain were subjected to diagnostic laparoscopy. Ages varied from 10 to 17 years. There were six males and seven females. Abdominal pain was present from 3 weeks to 12 months (mean, 2 months). Extensive laboratory and imaging studies did not contribute to the diagnosis. In all patients, the pain was disabling and	*OBJECTIVE:* Most pediatric emergency department (ED) visits are due to acute abdominal pain. Sonography is a reliable technique for differential diagnosis. The objective of this study was to re-appraise the role of sonography in evaluating acute abdominal pain in children. *METHODS:* Retrospective chart review of children aged <18 years with acute abdominal pain who visited the emergency department and underwent sonography between December 2004 and June 2006 was conducted. Patients with trauma were excluded. *FINDINGS:* 775 patients (478 males and 297 females, age 1-17 years; mean age 6±5.8 years)

			severe enough to warrant repeated visits to the pediatrician, emergency room visits, or hospital admissions, as well as absence from school. *RESULTS:* All children recovered uneventfully. Laparoscopic findings that identified the cause of abdominal pain were obtained in 12 of 13 patients. Laparoscopic appendectomy was done in all patients. There were no operative complications. One child presented three months later with incomplete small bowel obstruction, which resolved with conservative management. There were no other postoperative complications. Follow-up varied from six months to three years. Abdominal pain resolved in ten patients. One patient presented eight months later with biliary dyskinesia. She improved following laparoscopic cholecystectomy and later on sphincterotomy, but her pain has not yet completely resolved. One patient presented six months later with abdominal pain secondary to intestinal adhesions. Her pain completely resolved after laparoscopic lysis of adhesions. A third patient who developed lower abdominal pain six months after laparoscopy improved with conservative management and antibiotics for pelvic inflammatory disease. *CONCLUSIONS:* Diagnostic laparoscopy is a valuable procedure in the management of children with chronic recurrent abdominal pain. In the present study, laparoscopic examination revealed the cause of abdominal pain in most patients, and this pain resolved in most cases. Based on our experience, we recommend diagnostic laparoscopy early in the course of debilitating chronic recurrent abdominal pain in children. Appendectomy should be done when no other significant cause of abdominal pain has been identified, even if the appendix looks normal.	enrolled the study. Among 284 children with suspected appendicitis, 118 were diagnosed with appendicitis using sonography. Of 663 children without appendicitis, majority had gastrointestinal tract infection or non-specific abdominal pain. Other specific diagnoses were established by clinical, laboratory, and radiologic finings in 51 patients (including renal diseases in 20, intussusceptions in 15, gynecologic diseases in six, extra-abdominal disease in 4, and gastrointestinal tract abnormalities in 2). The sensitivity and specificity of sonography was 96.4% and 76.7%, respectively, for diagnosing appendicitis and 100% and 100%, respectively, for intussusception. *CONCLUSION:* Sonography remains a very effective, complementary, non-invasive method for evaluating children with acute abdominal pain, especially those with suspected appendicitis or intussusception.
21958104	20846301	0.542	*AIMS:* The objective of this study was to evaluate the cost-effectiveness of rivaroxaban versus the low-molecular-weight heparins (LMWH) enoxaparin and dalteparin for the prevention of venous thromboembolism (VTE) after total hip replacement and total knee replacement in Sweden. *METHODS:* The model included acute venous thromboembolic events and long-	*OBJECTIVES:* To estimate the cost-effectiveness of bortezomib (BTZ) compared with dexamethasone (DEX) and lenalidomide plus dexamethasone (LEN/DEX) for the treatment of relapsed/refractory multiple myeloma in Sweden. *METHODS:* We used partitioned survival analysis to assess survival data decomposed into three states: (i) alive before disease progression; (ii) alive after progression; and (iii) dead. The effects of treatment on

			term complications over a 5-year time horizon represented by an acute and a chronic phase with 1-year cycles. Transition probabilities were derived from the Regulation of Coagulation in Orthopaedic Surgery to Prevent Deep Vein Thrombosis and Pulmonary Embolism (RECORD) clinical trials. *RESULTS:* In patients undergoing total hip replacement, the incremental cost per additional quality-adjusted life-year of extended prophylaxis for 35 days with rivaroxaban versus 14 days of prophylaxis with enoxaparin or dalteparin was SEK29,400 and SEK35,400, respectively. In total knee replacement patients, 14 days of rivaroxaban dominated 14 days of LMWH as prophylaxis for VTE. *CONCLUSION:* The results of the economic model consistently showed that, over a 5-year period, rivaroxaban is a cost-effective alternative to 14 days of LMWH for VTE prophylaxis in Sweden.	time to progression and overall survival (OS) were obtained from published reports of the APEX, MM-009, and MM-010 randomized clinical trials. Costs included drug and administration costs, adverse events, treatment of relapses, and end-of-life costs. Utility estimates were derived from the literature. *RESULTS:* BTZ mean OS was 57.4 months compared with 44.6 and 54.1 months for DEX and LEN/DEX, respectively. Mean lifetime direct medical costs per patient were approximately 2010 SEK 1,904,462, 1,278,854, and 2,450,588 for BTZ, DEX, and LEN/DEX, respectively. Mean incremental cost per quality-adjusted life-year of BTZ compared to DEX was 2010 SEK 902,874 (€95,073) (95% CI: 514,791, 962,416) and was dominant with respect to LEN/DEX. *CONCLUSION:* BTZ and LEN/DEX are projected to prolong survival relative to DEX. From a Swedish perspective, BTZ is cost-effective compared to DEX and LEN/DEX.

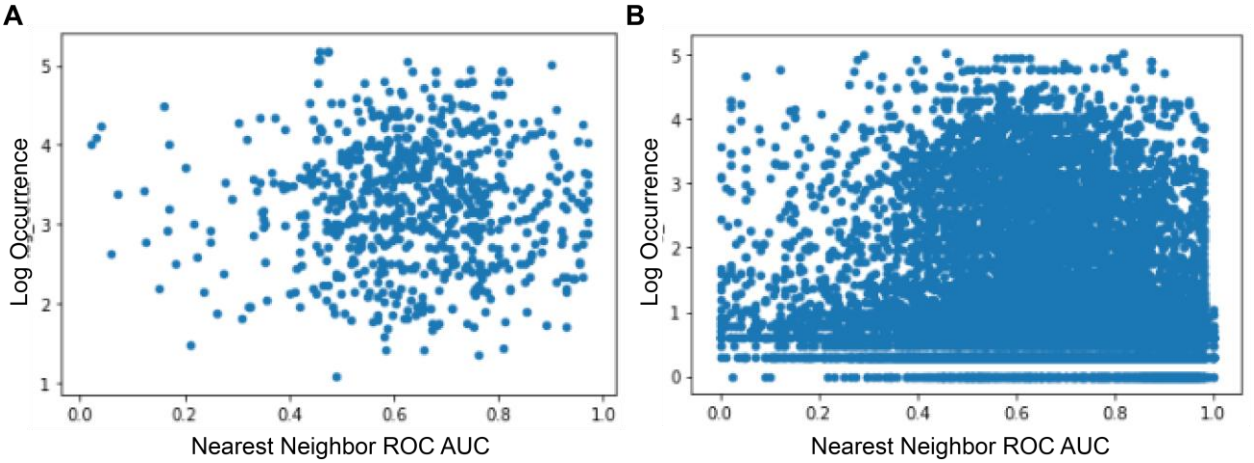

Supplemental Figure 1: Scatter plots of ROC AUC scores and $\log_{10}$ occurrence for compound-based nearest neighbor retrieval in Drugbank categorizations (A) and target associations (B).